Zero Image Watermarking Method Based on NSCT and Hadamard Transform

Jie Zhao

School of Electronic Information and Electrical Engineering, Shangluo University, Shangluo, Shaanxi, 726000, China

Corresponding author is Jie Zhao

Abstract

In order to improve the robustness and invisibility of image watermarking, this paper proposed a zero watermarking method based on nonsubsampled contourlet transform (NSCT) and Hadamard transform. After doing the nonsubsampled contourlet transform, the low frequent sub band was extracted. This sub band was divided into several blocks. Each block was implemented Hadamard transform. The Hadamard coefficients were used to obtain the construction image. The construction image and watermark were inputs of the cellular neural network, and the zero-watermarking registration image was the output. The image scrambling and cellular neural network improve the security and robustness. To deal with the scaling and rotation attacks, the scale-invariant feature transform (SIFT) was employed. The experimental results demonstrated the proposed method was robust to common image processing. This method is simple, and is convenient for real-time processing.

Keywords: ZERO WATERMARKING, NONSUBSAMPLED CONTOURLET TRANSFORM,; HADAMARD TRANSFORM, CELLULAR NEURAL NETWORK.

1. Introduction

With the development of multimedia technology and Internet, and the wide use of image processing software, it is becoming more and more convenient to modify and edit digital images. The advanced technology is primarily for the convenience of people, but also exposed a very obvious problem: the digital contents are much easier to be pirated or tampered. The image of copyright protection has become a social focus. In order to solve the copyright protection and content authentication problem, the digital watermark technology was proposed and got rapid development in recent years [1]. Generally, a good digital watermarking algorithm requires several important features of robustness, imperceptibly, small amount of computation, large embedding capacity and so on. The spatial domain algorithms are of the advantage of simplicity and high capacity, and the transform domain methods show more robustness. The balance of the watermarking imperceptibility and robustness is still a difficulty. Some methods optimize the embedding strength position or capacity using the machine learning. In [2], the watermark information was inserted into the middle frequency DCT coefficients. The neural network was used to obtain an automated system of creating maximum-strength watermarks. In [3], the feed-forward neural networks are used to embed and decode. Veysel Aslantas presented a novel watermarking method by virtue of genetic algorithm (GA) [4]. Modifications are optimized by GA to get the highest possible robustness and maintain the transparency. In [5], the parameters were used to embedding and extraction process, and genetic algorithm was applied for parameter optimization. Particle swarm optimization (PSO) algorithm was also adopted for watermarking in [6]. It was used to optimize the imperceptibleness and the carrier image quality. Recent years, the support vector machine (SVM) has

been used in the watermarking technology. Hong Peng et al. presented an image watermarking method based on SVM in multiwavelet domain [7]. The relation between the coefficients in various sub bands in discrete wavelet transform decomposition was used in [8]. Although these methods got a certain effect, but still have some limitations, such as "over learning" and so on.

Literature [9, 10] proposed zero-watermarking technique without modifying the original image. It includes the so called construction-registration and authentication procedures. In the registration procedure, the "constructed watermark" is generated using some image features and original watermark information, and is registered in the centralized authentication center. The authentication process is similar to traditional extraction process. The watermark information is recovered with recognition images and the data of authentication center. Since this idea need not modify the carrier image information, the imperceptibility is better, and the algorithms mainly focus on the robustness. In paper [11], a zero-watermarking was implemented in wavelet domain. The wavelet transform provides time-frequency and multistage analyze of the image. However, it couldn't represent the image effectively. Contourlet transform improved this problem. It is a novel multiresolution and directional expansion analysis of image using Pyramidal Directional Filter Bank (PDFB). Paper [12] proposed a novel zero watermarking method in Contourlet domain. The aliasing and leakiness of frequency spectrum was caused by the sampling in the transform procedure, then the nonsubsampled contourlet transform (NSCT) was presented by researchers.

In this paper, the algorithm gets the low-frequency sub image after NSCT. Then the Hadamard coefficients are used to generate the feature matrix. The scrambled watermark image and feature matrix are inputted into Cellular Neural Network, and the constructed image is produced. The watermark information can be extracted from the secret image and the scrambling key.

2. Nonsubsampled Contourlet Transform

The nonsubsampled contourlet transform is divided into two parts: the nonsubsampled pyramid (NSP) structure and the nonsubsampled directional filter bank (NSDFB) [13]. The NSDFB is constructed by eliminating down samples in the directional filter bank (DFB), and so as NSP. Fig. 1 shows the basic structure of NSDFB. This transform is composed of a bank of filters which separating the 2-D plane in the sub bands as shown in Fig. 1(b).

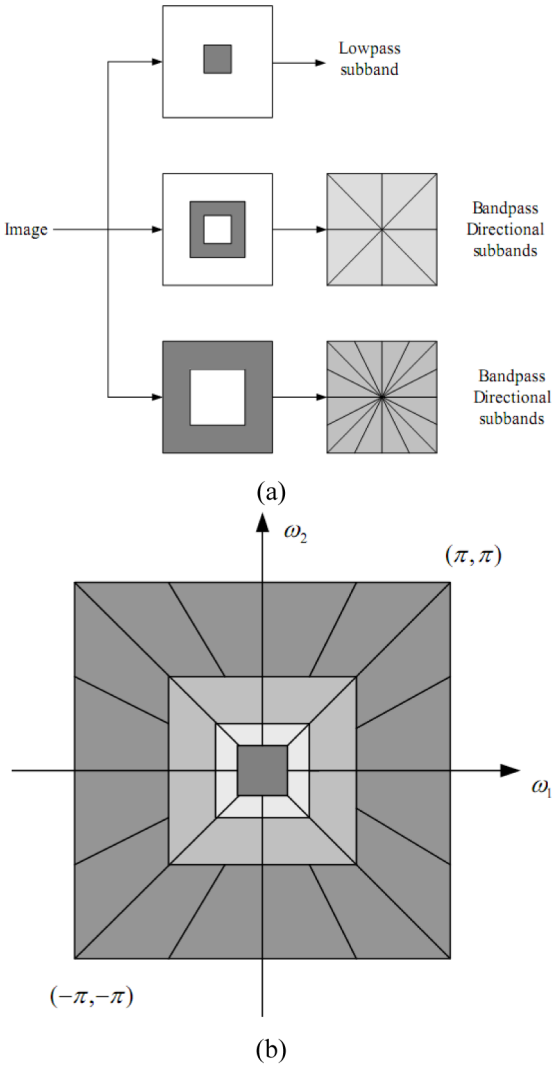

Figure 1. NSCT structure

The NSCT retains the advantages of Contourlet transform and suppresses the pseudo-Gibbs phenomenon at the same time.

3. Cellular Neural Network

Cellular Neural Network (CNN) simulated the non-liner and real-time speed array processor of VSLI at first, and has been used in many fields recent years [14]. For the 2-D CNN, the basic processing unit is called cells. Only neighboring cells can produce a role for each other. In image processing field, the CNN parallel processor can accomplish difference operations. For the M×N CNN array element, the mathematical model of each neuron operation can be described as following formula 1:

$$\dot{x} = -x_{ij} + \sum_{k,l\in N_r(i,j)} B_{k,l}u_{k,l} + \sum_{k,l\in N_r(i,j)} A_{k,l}y_{k,l} + I \qquad (1)$$

where $i = 1,2,\cdots M$, $j = 1,2,\cdots N$. x_{ij} is the current state of cell c_{ij}. $u_{k,l}$ and $y_{k,l}$ represent the network input and output. $N_r(i,j)$ denotes the r-neigh-

borhood of the cell c_{ij}. $A_{k,l}$ and $B_{k,l}$ are defined as the feedback template and control template, which are the coefficients linking cell to its neighbor. I denotes the threshold. The output equation can be described as:

$$y_{i,j} = \frac{1}{2}(|x_{i,j}+1| - |x_{i,j}-1|) \quad (2)$$

The relationship between the input $u_{k,l}$, the output $y_{k,l}$, and the state x_{ij} is determined by the feedback template A and the control template B as well as the threshold I.

By setting different templates and thresholds, the CNN parallel processor can realizes different image processing functions. For example, when $A=\begin{bmatrix}0&0&0\\0&2&0\\0&0&0\end{bmatrix}$, $B=\begin{bmatrix}0&0&0\\0&1&0\\0&0&0\end{bmatrix}$ and I = -1, it can realize the "and" operation.

4. Hadamard Transform

Two dimensional Hadamard transform matrix is a square matrix, which contains only 1 and -1. It is only needed to carry out the real number operation, the storage capacity is less than the general transformation, and the operation speed is much faster [15]. Two dimensional Hadamard transform and inverse transform kernels are given by equation 3 and 4:

$$g(x,y,u,v)=\frac{1}{N}(-1)^{\sum_{i=0}^{n=1}[b_i(x)b_i(u)+b_i(y)b_i(v)]} \quad (3)$$

$$h(x,y,u,v)=\frac{1}{N}(-1)^{\sum_{i=0}^{n=1}[b_i(x)b_i(u)+b_i(y)b_i(v)]} \quad (4)$$

Two dimensional Hadamard transformation and inverse transformation also have a similar form. It can be described by equation 5 and 6:

$$H(u,v)=\frac{1}{N}\sum_{x=0}^{N-1}\sum_{y=0}^{N-1}f(x,y)(-1)^{\sum_{i=0}^{n=1}[b_i(x)b_i(u)+b_i(y)b_i(v)]} \quad (5)$$

$$f(x,y)=\frac{1}{N}\sum_{x=0}^{N-1}\sum_{v=0}^{N-1}H(u,v)(-1)^{\sum_{i=0}^{n=1}[b_i(x)b_i(u)+b_i(y)b_i(v)]} \quad (6)$$

The minimal order (N = 2) Hadamard matrix is shown as equation 7:

$$\mathbf{H}_2=\begin{bmatrix}1&1\\1&-1\end{bmatrix} \quad (7)$$

Let $\mathbf{H}_N$ represents N order Hadamard matrix, and the relationship between the iterative calculation of higher-order Hadamard matrix is given the relationship between the iterative calculation of higher-order Hadamard matrix can be given by equation 8:

$$\mathbf{H}_{2N}=\begin{bmatrix}\mathbf{H}_N&\mathbf{H}_N\\\mathbf{H}_N&-\mathbf{H}_N\end{bmatrix} \quad (8)$$

It is only needed to carry out the real number operation, the storage capacity is less than the general transformation, and the operation speed is much faster.

5. Scale Invariant Feature Transform

As a powerful feature point diction algorithm, SIFT takes advantage of good invariance of image rotation, scaling and translation. It is used widely and also can correct the geometric distortion. The basic idea of SIFT is to get features by a series of filtering operation to extract stable point from image scale space. These feature points are detected both from undistorted and distorted image, and then the matched points are searched. In order to solve the scaling attack, the scale and central distance features of the matched points are used to calculate the scale distortion parameter, and then the scale distortion is restored. In the meantime, the SIFT central angles of the matched points are obtained to restore the rotated distortion [16]. The whole process can be described as:

(1) The function $L(x, y, \sigma)$ is defined for the image scale space. It can be obtained by the convolution of a variable-scale Gaussian function $G(x,y,\sigma)$ with an input image $I(x,y)$. It is given by equation 9:

$$L(x,y,\sigma)=G(x,y,\sigma)*I(x,y) \quad (9)$$

$D(x,y,\sigma)$ is utilized to locate the stable key point. The difference of two close scales detached using a multipartite parameter k is used to calculate $D(x,y,\sigma)$ and it is shown as formula 10:

$$D(x,y,\sigma)=L(x,y,k\sigma)-L(x,y,\sigma) \quad (10)$$

(2) The candidate feature points are selected, and the feature points of low contrast and the unstable edge response points are removed, so as to enhance the matching stability and improve the anti noise capability.

(3) Distribution direction of each feature point is implemented by the local image gradient direction. The gradient magnitude m and orientation θ are given by formula 11 and 12:

$$m=\sqrt{(L(x+1,y)-L(x-1,y))^2+(L(x,y+1)-L(x,y-1))^2} \quad (11)$$

$$\theta=\tan^{-1}\left(\frac{L(x,y+1)-L(x,y-1)}{L(x+1,y)-L(x-1,y)}\right) \quad (12)$$

(4) The stable SIFT feature vectors are generated, and they can be used to correct the scaling and rotation distortions. If the image is scaled s times, the number of matching points is n, the scale factor of

key point P_i in the original image is d_i, and the scale factor of the corresponding matching key point Q_i in the scaled image is q_i, then we can get s by equation 13:

$$s = (\sum_{i=1}^{n} q_i / d_i) / n \quad (13)$$

If the rotated angle is α, the number of matching points is n, the center angle of key point P_i in the original image is ϕ_i, and the center angle of the corresponding matching key point Q_i in the rotated image is φ_i, then we can get α by equation 14:

$$\alpha = (\sum_{i=1}^{n} (\varphi_i - \phi_i)) / n \quad (14)$$

6. Watermarking Method

Let $f(i, j)$ denote the original carrier image and $w(x, y)$ denote binary watermarking image.

Construction process:

(1) The original watermark $w(x, y)$ is scrambled by secret key, and produced $w'(x, y)$.

(2) One level nonsubsampled contourlet transform is used to decompose the original host image.

(3) The low-frequency sub band is divided into blocks, such as 8×8. For each block, the Hadamard transform is implemented, and the direct-current coefficient is denoted as $d(x, y)$. Then the mean value of all the DC coefficients is denoted as d.

(4) The construct matrix $C(x, y)$ is generated by the following rule:

if $d(x, y) > d$,
then $C(x, y)$=1;
else $C(x, y)$=0.

(5) The scrambled watermark image $w'(x, y)$ and construct matrix $C(x, y)$ are the inputs of CNN network. The output is the so called constructed watermark $S(x, y)$, it also the registration information of this zero watermarking method. $S(x, y)$ can be scrambled in order to enhance the system security.

Extraction process:

(1) One level nonsubsampled contourlet transform is employed to decompose the test image $f'(i, j)$. If the watermarked image suffered scaling or rotation attack, the geometric correction by SIFT should be done firstly.

(2) The low-frequency sub band of $f'(i, j)$ is divided into same blocks according to the construction process. For each block, the Hadamard transform is implemented, and the direct-current coefficient is denoted as $d'(x, y)$. Then the mean value of all the DC coefficients is denoted as d'.

(3) The construct matrix $C'(x, y)$ is generated by the following rule:

if $d'(x, y) > d'$,
then $C'(x, y)$=1;
else $C'(x, y)$=0.

(4) The registration information $S(x, y)$ and construct matrix $C(x, y)$ are the inputs of CNN network. The output is denoted as $w'_a(x, y)$. The extracted watermark $w_a(x, y)$ can be generated by the secret key.

(5) The watermark is determined by the correlation coefficient (Similarity) between the original watermark $w(x, y)$ and the extracted watermark $w_a(x, y)$.

The correlation coefficient NC can be computed as equation 15:

$$NC = \frac{\sum_x \sum_y w(x, y) w_a(x, y)}{\sqrt{\sum_x \sum_y w^2(x, y)} \sqrt{\sum_x \sum_y w_a^2(x, y)}} \quad (15)$$

If the value of NC is bigger than the empirical threshold value, the watermarking information exists. If not, the watermarking information does not exist.

7. Experimental Simulation

For this experiment, Matlab 7.5 was used as the software platform. The gray image "lena" was adopted as the original carrier image, and one binary image was used as the original watermark image. Fig. 2 shown the original carrier image, original watermark, and Fig. 3 shown the watermarked image and extracted watermark from the watermarked image.

Figure 2. Original image and watermark

Figure 3. Watermarked image and extracted watermark

Then the robustness test of this method was implemented. The watermarked image was attacked and the NC values were recorded. Results for common image processing operations were shown in Table 1.

Table 1. Results of common attacks

Attacks	This method	Method in [12]
Salt and pepper noise(0.01)	0.9444	0.9394
Salt and pepper noise(0.02)	0.9413	0.9016
Gaussian noise(0, 0.001)	0.9754	0.9670
Gaussian noise(0, 0.002)	0.9711	0.9443
Median filtering(3×3)	0.9902	0.9736
Median filtering(5×5)	0.9539	0.9601
Cropping 1/16	0.8058	0.9022
JPEG Compression (Q=50)	0.9855	0.9813
JPEG Compression (Q=20)	0.9711	0.9668
JPEG Compression (Q=10)	0.9496	0.9238
Scaling(1.1)	0.9454	Fail
Rotation(10°)	1.0000	Fail
Rotation(20°)	0.9186	Fail

In order to obtain the visual effect, the partial results with average filtering, Gaussian noise, and speckle noise are given. These results were shown in Fig. 4, Fig. 5 and Fig. 6.

According to the test results, most of the values of correlation coefficient distribute between 0.9-1. This shows the robustness to usual attacks of this method. This method performs better than the contourlet domain algorithm in [12], but the ability to resist cropping attack still needs to be strengthened.

Conclusions

This paper presented a novel zero image watermarking algorithm based on Hadamard and nonsubsampled contourlet transform. The registration image was generated through the cellular neural network, and the security is higher. Since the Hadamard transform operation is simple, and the parallel processing of cellular neural network is easy to be implemented, this algorithm can be applied to the occasion with high real-time requirements. Although the zero watermarking is a breakthrough in the conventional watermarking method, this idea is still to be further studied in order to make it feasible and practical.

Figure 4. Average filtering(3×3), NC=0.9626

Figure 5. Gaussian noise(0, 0.002) NC=0.9711

Figure 6. Speckle noise(0.01) NC=0.9575

Acknowledgements

Supported by the Scientific Research Foundation of the Science and Technology Department of Shaanxi Province (Program No. 2014JM2-6122).

References

1. Rakesh Ahuja, S. S. Bedi, Himanshu Agarwal. A Survey of Digital Watermarking Scheme. MIT International Journal of Computer Science and Information Technology, 2012, 2(1), pp. 52-59.
2. S. Oueslati, A. Cherif, B. Solaimane. Adaptative image watermarking scheme based on neural network. International Journal of Engineering Science and Technology, 2011, 3(1), pp. 748-756.
3. A. A. Sirota, M. A. Uchenko, E. Y. Mitrofanova, et al. Digital watermarking based on neural network technologies. Journal of Convergence Information Technology, 2013, 8(11), pp. 616-624.
4. Veysel Aslantas. A singular-value decomposition-based image watermarking using genetic algorithm. AEU-International Journal of Electronics and Communications, 2008, 62(5), pp. 386-394.
5. K. Ramanjaneyulu, K. Rajarajeswari. Wavelet-based oblivious image watermarking scheme using genetic algorithm. Iet Image Processing, 2012, 6(4), pp. 364-373.
6. A. I. Hammouri, B. Alrifai, H. Al-Hiary. An intelligent watermarking approach based particle swarm optimization in discrete wavelet domain. International Journal of Computer Science Issues, 2013, 10(2), pp. 330-338.

7. Hong Peng, Jun Wang, Weixing Wang. Image watermarking method in multiwavelet domain based on support vector machines. Journal of Systems and Software, 2010, 83(8), pp. 1470–1477.
8. B. Jagadeesh, P. R. Kumar, P. C. Reddy. Robust digital image watermarking scheme in discrete wavelet transform domain using support vector machines. International Journal of Computer Applications, 2013, 73(14), pp. 1-7.
9. Ye Dengpan. New zero-watermark copyright protection scheme based on binary bitmap. Application Research of Computers, 2007, 24(8), pp. 239-241.
10. Baoru Han, Lisha Cai, Wenfeng Li. Zero-watermarking algorithm for medical volume data based on legendre chaotic neural network and perceptual hashing. International Journal of Grid and Distributed Computing, 2015, 8(1), pp. 201-212.
11. Zhang Xiao-peng, Tong Xiao-hua, Liu Miao-long. A new zero-watermark algorithm based on chaotic sequences and wavelet transform. Geomatics and Spatial Information Technology, 2010, 33(1), pp. 156-160.
12. Zeng Fan-juan, Zhou An-ming. Image zero watermarking algorithm based on contourlet transform and singular value decomposition. Journal of Computer Applications, 2008, 28(8), pp. 2033-2035.
13. Jun Wang, Jinye Peng, Xiaoyi Feng, et al. Image fusion with nonsubsampled contourlet transform and sparse representation. Journal of Electronic Imaging, 2013, 22(4), pp. 6931-6946.
14. M. Duraisamy, S. Duraisamy. A technique for tumor region identification using cellular neural network. Journal of Theoretical and Applied Information Technology, 2013, 55(1), pp. 1-13.
15. Fenghua Wang, Hui Xie, Zhitao Huang. Blind reconstruction of convolutional code based on segmented Walsh-Hadamard transform. Journal of Systems Engineering and Electronics, 2014, 25(5), pp. 748-754.
16. Li Zhen-hong, Wu Hui-zhong. Geometric distortion correction algorism based on SIFT for image watermarking. Computer Engineering and Design, 2008, 29(12), pp. 3215-3217.

Comparison between Fully Bayesian Hierarchical Meta-analysis and Classical Meta-analysis: A Monte Carlo Study Based on Correlation Coefficient

Wei CHEN[12], Shouying ZHAO[2], Ying GE[1], Jie LUO[2], Jinfu ZHANG[1]*

[1] Faculty of Psychology, Southwest University, Chongqing, 400715, China
[2] Department of Educational Science, Guizhou Normal University, Guiyang, 550001, China

Abstract
Take the Pearson's correlation coefficient as an example, the difference between fully Bayesian hierarchical meta-analysis and classical meta-analysis was compared. Through the experimental design of following four factors